Analysis of a Thin Slot Discontinuity in the Reference Plane of a Microstrip Structure

Ammar B. Kouki, *Member, IEEE,* Raj Mittra, *Fellow, IEEE,* and Chi Hou Chan, *Member, IEEE*

***Abstract*—This paper presents a perturbational approach based upon the spectral domain technique for the analysis of the discontinuity effects introduced by a thin slot in the ground plane of a microstrip line. The discontinuity problem is formulated in terms of the unknown slot field by using the notion of equivalent half-space problems, using a new rigorous procedure for deriving the TE–TM decomposition of the fields and equivalent transmission line models. The perturbation current on the infinite microstrip is computed once the electric field in the slot has been derived, and an equivalent circuit for the discontinuity is obtained from this perturbation current for the low-frequency regime. Computed results are presented and compared to the measured data.**

I. Introduction

OVER the past several years, considerable attention has been devoted to the problem of characterizing microstrip discontinuities, and a number of different approaches have been employed to investigate them. These approaches include: static and quasi-static methods [1]–[6], which are applicable in the low-frequency regime and are based on the modeling of the discontinuity by equivalent lumped circuit elements; more accurate waveguide models [7]–[9], which incorporate the frequency-dependent properties of the discontinuities; and rigorous full-wave analyses, such as the mode matching technique [10], [11] or the spectral domain approach [12]–[15], both of which provide more accurate results over a wide frequency range. While the more common discontinuities, e.g., bends and step discontinuities, have been studied rather extensively, one discontinuity that has received little attention in the literature is that of the thin slot in the ground plane of a microstrip line.

Although considerable work has been done in investigating the comparable geometries of microstrip-fed slot antennas [16]–[20], no analysis is available for the discontinuity effects of a thin slot. This is understandable since one of the primary objectives in the antenna design is to have an efficient radiator by maximizing the amount of energy coupled from the microstrip to the slot. However, in many circuits, slots may be present not for radiation purposes but rather to provide other functions such as allowing vias to run through them, and facilitating the mechanical support. In such cases, the radiation effects are generally expected to be small, and the primary concern is then the unavoidable perturbational effects on the microstrip current. This intuitive description must be backed by a rigorous electromagnetic analysis, not only to verify it, but also to study the range of its validity as one expects the effects of the discontinuity to be more prominent at higher frequencies.

In this paper, a spectral domain-based perturbational approach is used to analyze the discontinuity effects due to the presence of a thin slot in the ground plane of a microstrip line. This approach comprises the following five steps.

1) Initially, the microstrip currents are assumed to be those of the unperturbed geometry, i.e., in the absence of the slit. These original currents, along with the dominant mode's propagation constant, can be obtained by following the method described in [21].

2) Next, the results of the previous step are used to compute the slot's electric field. This is done through a procedure where equivalent half-space problems are constructed, a TE-y–TM-y decomposition of the fields is applied along with equivalent transmission line models to derive expressions for the dyadic Green's function, and the continuity of the tangential magnetic field in the slot is enforced in a Galerkin procedure to yield the desired matrix equation.

3) Once the slot's electric field is obtained, it is then used as the source of the incident field for calculating the perturbation current on the strip.

4) The original microstrip currents are replaced by the perturbation currents of step 3 and the process is iterated until convergence.

5) After convergence, the scattering parameters of the discontinuity are computed from the resulting current distribution.

II. Formulation

Fig. 1 depicts the geometry of the slit discontinuity to be analyzed. The ground plane is taken to coincide with the x-z plane, and is assumed to extend infinitely in both of these directions. The substrate material is assumed to be isotropic and nonmagnetic, but may have an arbitrary complex permittivity. All conductors are assumed to be infinitely conducting and to have zero thickness. The solution process consists of two main phases: the computation of the slot's electric field given a microstrip current, and the determination of the perturbation current induced on the strip given an electric field distribution in the slot.

Manuscript received August 7, 1992; revised December 21, 1992.

A. B. Kouki is with the Microwave Research Laboratory, Electrical and Computer Engineering Department, Ecole Polytechnique de Montreal, Montreal, P.Q., Canada H3C 3A7.

R. Mittra is with the Electromagnetic Communication Laboratory, University of Illinois, 1406 W. Green St., Urbana, IL 61801.

C. H. Chan is with the Electrical Engineering Department, University of Washington, Seattle, WA 98195.

IEEE Log Number 9210217.

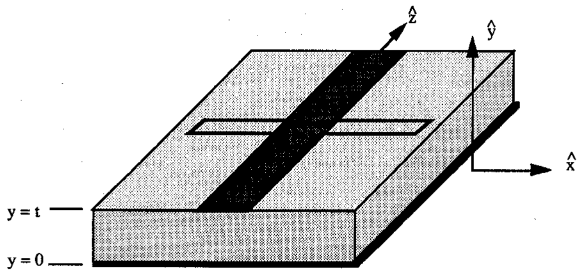

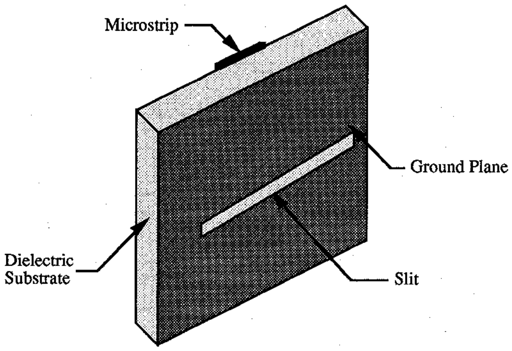

Fig. 1. Geometry of the thin slot discontinuity in the ground plane of a microstrip line.

A. The Electric Field in the Slot

The initial microstrip current is easily obtained from a spectral domain analysis such as the one described in [21]. To compute the slot's electric field due to a given microstrip current, a procedure similar to [22] is followed whereby the original problem is decomposed in two equivalent half-space ones. This is accomplished by first shorting the aperture and then restoring its electric field by an equivalent magnetic current radiating in the presence of the shorted plane, see Fig. 2. Next, individual expressions for the magnetic field on each side of the conducting plane are written in the general form

$$\vec{H} = \vec{H}_m + \vec{H}_i \tag{1}$$

where $\vec{H}_m$ denotes the magnetic field produced by the equivalent magnetic current (scattered field) while $\vec{H}_i$ represents the incident magnetic field due to the strip current radiating in the presence of the shorted plane (present only in the $y > 0$ half-space). Finally, the desired integral equation is obtained by imposing the continuity of the tangential magnetic field through the slot.

First, consider the scattered field term. For the ith homogeneous, source-free region in a given half-space, the electromagnetic fields can be written in terms of an electric vector potential as

$$\vec{H}^i_m = -j\omega\varepsilon_i\vec{F}^i + \frac{1}{j\omega\mu}\nabla\left(\nabla\bullet\vec{F}^i\right) \quad \text{and} \quad \vec{E}^i_m = -\nabla\times\vec{F}^i. \tag{2}$$

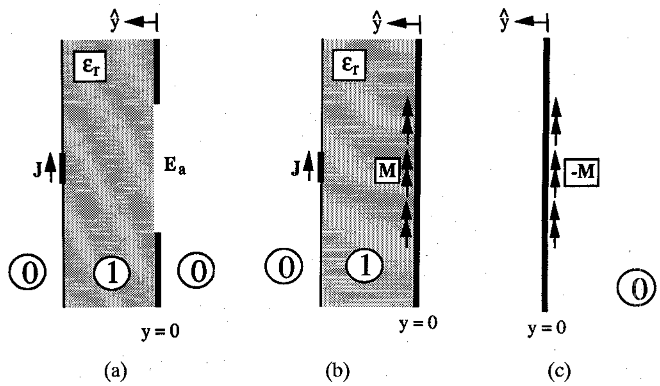

Fig. 2. Construction of the equivalent half-space problems. (a) Original problem, valid everywhere; (b) equivalent left-half-space problem, valid for $y > 0$ only; (c) equivalent right-half-space problem, valid for $y < 0$ only.

Defining the electric vector potential $\vec{F}^i$ as

$$\vec{F}^i(\vec{r},\vec{r}\,') = \int\!\!\int G^i(\vec{r},\vec{r}\,')\vec{M}(\vec{r}\,')\,d\vec{r}\,' \tag{3a}$$

with

$$G^i(\vec{r},\vec{r}\,') = \frac{e^{-jk_i/\vec{r}-\vec{r}\,'/}}{4\pi/\vec{r}-\vec{r}\,'/} \quad \text{and}$$
$$\vec{M}(\vec{r}\,') = M_x(\vec{r}\,')\hat{x} + M_z(\vec{r}\,')\hat{z} \tag{3b}$$

and using the Fourier transform given by the pair

$$\begin{cases} \tilde{F}(\alpha,\beta) = \int_{-\infty}^{\infty}\int_{-\infty}^{\infty} f(x,z)e^{-j(\alpha x+\beta z)}\,dx\,dz \\ f(x,z) = \frac{1}{4\pi^2}\int_{-\infty}^{\infty}\int_{-\infty}^{\infty}\tilde{F}(\alpha,\beta)e^{j(\alpha x+\beta z)}\,d\alpha\,d\beta \end{cases} \tag{4}$$

equation (2) yields the following expressions for the electric and magnetic fields in the transform domain:

$$\begin{cases} \tilde{E}^i_x = -\frac{\partial(\tilde{G}^i\tilde{M}_z)}{\partial y} \\ \tilde{E}^i_y = j\left[\alpha\tilde{M}_z - \beta\tilde{M}_x\right]\tilde{G}^i \\ \tilde{E}^i_z = \frac{\partial(\tilde{G}^i\tilde{M}_x)}{\partial y} \end{cases}$$
$$\begin{cases} \tilde{H}^i_x = -j\omega\varepsilon_i\tilde{G}^i\tilde{M}_x - \frac{1}{j\omega\mu}\left[\alpha\left(\alpha\tilde{M}_x + \beta\tilde{M}_z\right)\tilde{G}^i\right] \\ \tilde{H}^i_y = \frac{1}{\omega\mu}\left[\frac{\partial}{\partial y}\left\{\left(\alpha\tilde{M}_x + \beta\tilde{M}_z\right)\tilde{G}^i\right\}\right] \\ \tilde{H}^i_z = -j\omega\varepsilon_i\tilde{G}^i\tilde{M}_z - \frac{1}{j\omega\mu}\left[\beta\left(\alpha\tilde{M}_x + \beta\tilde{M}_z\right)\tilde{G}^i\right] \end{cases} \tag{5}$$

where the spatial derivatives $\frac{\partial}{\partial x}$ and $\frac{\partial}{\partial z}$ have been replaced by $j\alpha$ and $j\beta$, respectively, by virtue of the Fourier transform property. It can now be easily seen that a TE–TM decomposition of the fields with respect to the y-axis is readily obtainable by setting the equations for y-components of the electric and magnetic fields in (5) equal to zero. Thus, for a given spectral component specified by its (α,β) values, an arbitrary surface magnetic current $\vec{\tilde{M}}$ can be written as

$$\vec{\tilde{M}} = \tilde{M}_{e1}\hat{e}_1 + \tilde{M}_{e2}\hat{e}_2 \tag{6}$$

with $\tilde{M}_{e2}$ producing the TE-y fields while $\tilde{M}_{e1}$ gives the TM-y components. The new components $\tilde{M}_{e1}$ and $\tilde{M}_{e2}$ are given by

$$\begin{cases} \beta\tilde{M}_x - \alpha\tilde{M}_z = \tilde{M}_{e1} \\ \alpha\tilde{M}_x + \beta\tilde{M}_z = \tilde{M}_{e2} \end{cases} \tag{7}$$

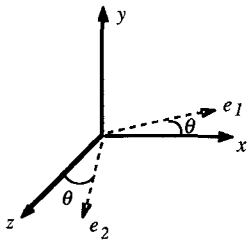

Fig. 3. Coordinate transformation for the TE–TM decomposition of the fields.

and the unit vectors $\hat{e}_1$ and $\hat{e}_2$ are related the $(\hat{x}, \hat{z})$ coordinate system by (see Fig. 3)

$$\begin{bmatrix} \hat{e}_1 \\ \hat{e}_2 \end{bmatrix} = \begin{bmatrix} \cos\theta & -\sin\theta \\ \sin\theta & \cos\theta \end{bmatrix} \begin{bmatrix} \hat{x} \\ \hat{z} \end{bmatrix} \tag{8}$$

with $\sin\theta = \alpha/\sqrt{\alpha^2+\beta^2}$ and $\cos\theta = \beta/\sqrt{\alpha^2+\beta^2}$. From (5) and (7), one can show that the TE-y fields are $\{\tilde{H}_y^i, \tilde{E}_{e1}^i, \tilde{H}_{e2}^i\}$ and the TM-y components are $\{\tilde{E}_y^i, \tilde{H}_{e1}^i, \tilde{E}_{e2}^i\}$. Note that (7) and (8) are similar to those given in [21] but, because of the duality of the current source and the choice of potential in (2-3), $(\hat{e}_1, \hat{e}_2)$ are equivalent to $(-u, v)$ in [21].

Next, writing Maxwell's curl equations in the $(\hat{e}_1, \hat{e}_2)$ coordinate system and using the above TE–TM decomposition, one obtains

$$\text{TE} - y \begin{cases} \dfrac{\partial \tilde{E}_{e1}^i}{\partial y} = j\omega\mu \tilde{H}_{e2}^i \\ \dfrac{\partial \tilde{H}_{e2}^i}{\partial y} = \dfrac{\gamma_i^2}{j\omega\mu}\tilde{E}_{e1}^i \end{cases} \quad \text{and}$$

$$\text{TM} - y \begin{cases} \dfrac{\partial \tilde{H}_{e1}^i}{\partial y} = -j\omega\varepsilon_i \tilde{E}_{e2}^i \\ \dfrac{\partial \tilde{E}_{e2}^i}{\partial y} = -\dfrac{\gamma_i^2}{j\omega\varepsilon_i}\tilde{H}_{e1}^i \end{cases} \tag{9}$$

where $\gamma_i^2 = \alpha^2 + \beta^2 + \varepsilon_{ri}k_0^2$. These equations are equivalent to the telegraphist equations with $\tilde{E} \leftrightarrow V$ and $\tilde{H} \leftrightarrow I$. With this equivalence, electric surface currents at a given y location are represented by a shunt current source, while magnetic surface currents (aperture electric fields) are equivalent to series voltage sources. Therefore, the analysis of the original field problem can now be converted to one of the solution of simple transmission line circuits. Hence, using the transmission line models for the TE–TM fields and the coordinate transformation of (8), the tangential components of the scattered magnetic field on either side of the slot $(y = 0^{\pm})$ are written as

$$\begin{bmatrix} \tilde{H}_x^m \\ \tilde{H}_z^m \end{bmatrix}_{0^+} = \begin{bmatrix} Y_h^+ \sin^2\theta + Y_e^+ \cos^2\theta & \sin\theta\cos\theta(Y_h^+ - Y_e^+) \\ \sin\theta\cos\theta(Y_h^+ - Y_e^+) & Y_e^+ \sin^2\theta + Y_h^+ \cos^2\theta \end{bmatrix} \cdot \begin{bmatrix} \tilde{M}_x \\ \tilde{M}_z \end{bmatrix} \tag{10}$$

and

$$\begin{bmatrix} \tilde{H}_x^m \\ \tilde{H}_z^m \end{bmatrix}_{0^-} = \begin{bmatrix} Y_h^- \sin^2\theta + Y_e^- \cos^2\theta & \sin\theta\cos\theta(Y_h^- - Y_e^-) \\ \sin\theta\cos\theta(Y_h^- - Y_e^-) & Y_e^- \sin^2\theta + Y_h^- \cos^2\theta \end{bmatrix} \cdot \begin{bmatrix} -\tilde{M}_x \\ -\tilde{M}_z \end{bmatrix} \tag{11}$$

where

$$\begin{cases} Y_h^+ = Y_{te}^1 \dfrac{Y_{te}^1 + Y_{te}^0 \coth\gamma_1 t}{Y_{te}^0 + Y_{te}^1 \coth\gamma_1 t} \\ Y_e^+ = Y_{tm}^1 \dfrac{Y_{tm}^1 + Y_{tm}^0 \coth\gamma_1 t}{Y_{tm}^0 + Y_{tm}^1 \coth\gamma_1 t} \end{cases} \quad \text{and} \quad \begin{cases} Y_h^- = Y_{te}^0 \\ Y_e^- = Y_{tm}^0 \end{cases} \tag{12}$$

with $Y_{te}^i = \gamma^i/(j\omega\mu)$ and $Y_{tm}^i = j\omega\varepsilon_i/(\gamma_i)$.

Similarly, the spectral decomposition described above can be used to derive an expression for the incident magnetic field at the plane of the slot. Again, this field is produced by the microstrip currents in the presence of a shorted ground plane. Note that because of the duality of the source, J_{e1} produces the TE-y fields, while J_{e2} is associated with the TM-y fields, so that

$$\begin{bmatrix} \tilde{H}_x^i \\ \tilde{H}_z^i \end{bmatrix}_{0^+} = \begin{bmatrix} \sin\theta\cos\theta(Y_h' - Y_e') & Y_h' \sin^2\theta\cos\theta - Y_e' \cos^2\theta \\ Y_e' \cos^2\theta + Y_h' \sin^2\theta & \sin\theta\cos\theta(Y_h' - Y_e') \end{bmatrix} \cdot \begin{bmatrix} \tilde{J}_x \\ \tilde{J}_z \end{bmatrix} \tag{13}$$

with

$$\begin{cases} Y_h' = \dfrac{Y_{te}^1 / \sinh\gamma_1 t}{Y_{te}^0 + Y_{te}^1 \coth\gamma_1 t} \\ Y_e' = \dfrac{Y_{tm}^1 / \sinh\gamma_1 t}{Y_{tm}^0 + Y_{tm}^1 \coth\gamma_1 t} \end{cases} . \tag{14}$$

Finally, the boundary condition on the total tangential magnetic field must be enforced. In the spatial domain, this condition reads

$$\iint_{\text{aperture}} \vec{H}_t^+ \cdot \vec{P}\, dx\, dz = \iint_{\text{aperture}} \vec{H}_t^- \cdot \vec{P}\, dx\, dz. \tag{15}$$

Invoking Parseval's equality, (15) yields

$$\int_{-\infty}^{\infty}\int_{-\infty}^{\infty} \vec{\tilde{H}}_t^+ \cdot \vec{\tilde{P}}^* \, d\alpha\, d\beta = \int_{-\infty}^{\infty}\int_{-\infty}^{\infty} \vec{\tilde{H}}_t^- \cdot \vec{\tilde{P}}^* \, d\alpha\, d\beta. \tag{16}$$

This equation is then solved using a moment method approach.

B. The Perturbation Current

Denoting the unknown perturbation current as $\vec{J}^p$, the scattered electric field associated with it, $\vec{E}^{sp}$, can be written as

$$\vec{E}^{sp} = \vec{E}_j^{sp} + \vec{E}_m^{sp}. \tag{17}$$

The incident field term, $\vec{E}_m^{sp}$, is provided by the magnetic current of the aperture. It is evaluated at $y = t$ in the absence of the conducting strip, and is similar in form to (10) and

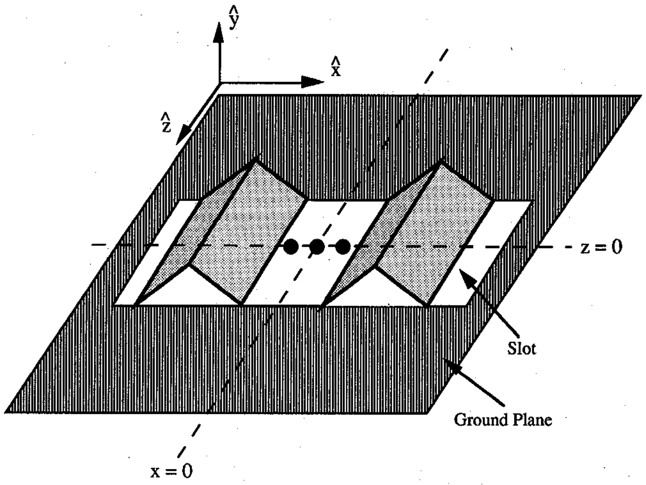

Fig. 4. Basis functions for expanding the z-directed aperture electric field.

(11). Enforcing the boundary condition on the total tangential electric field on the strip gives

$$\int_{strip} \vec{E}_j^{sp} \cdot \vec{P}\, dx\, dz = -\int_{strip} \vec{E}_m^{sp} \cdot \vec{P}\, dx\, dz. \tag{18}$$

Again, using Parseval's equality, the transform domain version of (18) reads

$$\int_{-\infty}^{\infty}\int_{-\infty}^{\infty} \tilde{\vec{E}}_j^{sp} \cdot \tilde{\vec{P}}^{*}\, d\alpha\, d\beta = -\int_{-\infty}^{\infty}\int_{-\infty}^{\infty} \tilde{\vec{E}}_m^{sp} \cdot \tilde{\vec{P}}^{*}\, d\alpha\, d\beta. \tag{19}$$

Equation (19) is then solved using the moment method.

III. Numerical Implementation and Results

All the results presented in this section are for a microstrip structure with a dielectric constant of 4.7, a dielectric height of 31 mils, and strip width of 55 mils giving a 50 Ω line. Also, the following simplifying assumptions have been made.

1) The slot is thin in the z-direction. Therefore, the x-directed aperture electric field can be neglected with good accuracy. Consequently, only M_x is retained as the unknown in (10), (11), and (16).

2) The x-directed electric current on the strip is neglected. This approximation is good for the relatively low frequencies considered here (1–3 GHz) where the strip width is a small fraction of the wavelength.

3) The dominant mode is assumed to be the only mode propagating in the structure.

In the moment method solution of (8), the aperture electric field is expanded in terms of a set of roof-top basis functions as shown in Fig. 4. The number of such basis functions is chosen so as to ensure that a minimum of 10 per dielectric region wavelength are used. Using Galerkin testing, a matrix equation is set up and solved for the aperture field distribution. Figs. 5 and 6 present the magnitude and phase of such distributions for a 10 cm (in x) by 5 mm (in z) slot at 1, 2, and 3 GHz.

In computing the induced strip current from the slot's aperture field, care must be taken in choosing the expansion and testing functions because the strip is assumed to be of

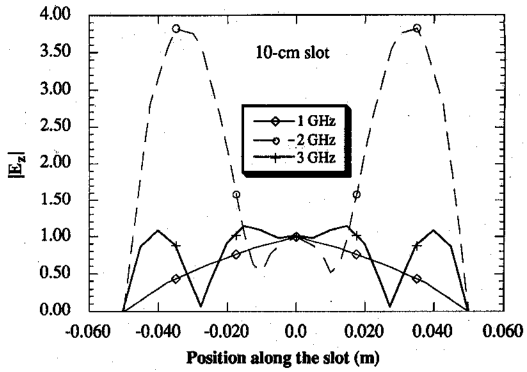

Fig. 5. Magnitude of the z-directed electric field in a 10-cm slot at different frequencies.

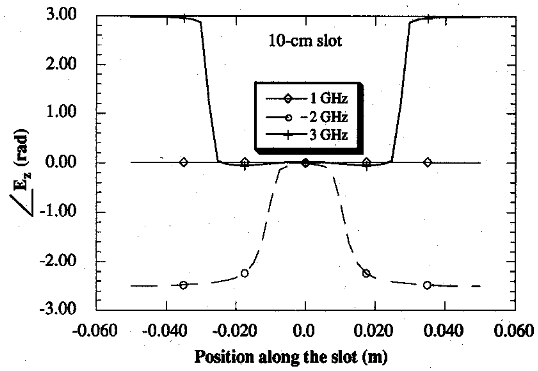

Fig. 6. Phase of the z-directed electric field in a 10-cm slot at different frequencies.

infinite extent in the z-direction. A good choice for such functions is described in [14] and [23], where it has been applied to the various discontinuities. Here, with the above assumptions, the induced current can be expanded in the form

$$\begin{cases} J_z^+(x,z) = T\left[\zeta_{e1}(x,s)\{f_1^+(z) - jf_2^+(z)\}\right] \\ J_z^-(x,z) = R\left[\zeta_{e1}(x,s)\{f_1^-(z) + jf_2^-(z)\}\right] \end{cases} \tag{20}$$

where T and R represent the transmission and reflection coefficients, respectively. In terms of scattering parameters, R represents S_{11} while T corresponds to S_{21}. The x- and z-dependencies in (20) are as follows:

$$\zeta_{ei}(x,\tau) = \frac{\cos[(i-1)\pi(1+x/\tau)]}{\sqrt{1-(x/\tau)^2}} \tag{21}$$

and

$$\begin{cases} f_1^+(z) = \cos(\beta_o z) & \lambda_o/4 < z < (\nu + 1/4)\lambda_o \\ f_2^+(z) = \sin(\beta_o z) & 0 < z < \nu\lambda_o \\ f_1^-(z) = \cos(\beta_o z) & -(\nu + 1/4)\lambda_o < z < -\lambda_o/4 \\ f_2^-(z) = \sin(\beta_o z) & -\nu\lambda_o < z < 0 \end{cases} \tag{22}$$

with t being the width of the strip, β_o the dominant mode's propagation constant, λ_o the dominant mode's wavelength, and n an integer. Note that the truncation used above and shown in Fig. 7 ensures that no artificial discontinuity is introduced since all functions start from zero and go to zero at their truncation points.

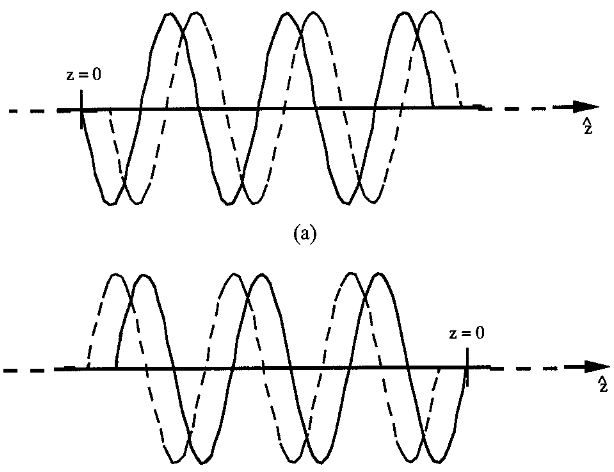

Fig. 7. Basis functions for expanding the induced z-directed microstrip current. (a) Truncation scheme for $z > 0$: ----, —— imaginary part; (b) truncation scheme for $z < 0$: ----, —— imaginary part.

The Fourier transform of (20) is given by

$$\begin{cases} \tilde{J}_z^+(\alpha,\beta) = T\left[\tilde{\zeta}_{e1}(\alpha,s)\left\{\frac{\beta_o}{\beta_o^2-\beta^2}\left(e^{-j\beta\nu\lambda_o}-1\right)\left(e^{-j\beta\lambda_o/4}+j\right)\right\}\right] \\ \tilde{J}_z^-(\alpha,\beta) = R\left[\tilde{\zeta}_{e1}(\alpha,s)\left\{\frac{\beta_o}{\beta_o^2-\beta^2}\left(e^{j\beta\nu\lambda_o}-1\right)\left(e^{j\beta\lambda_o/4}+j\right)\right\}\right]. \end{cases} \tag{23}$$

It can be shown, using l'Hosipital's rule, that both expressions in (23) approach finite limits as $\beta \to \pm\, \beta_o$ and the singularity problem is avoided. However, the exponential terms in (23) give rise to highly oscillatory integrands that present a serious numerical difficulty when evaluating the inner products by numerical integration. Furthermore, the rate of oscillation becomes higher as the basis functions are truncated at distances farther away from the slot (i.e., as ν becomes larger). To avoid compounding this problem, a non-Galerkin testing procedure is employed by choosing pulse testing functions that extend from 0 to $(\nu + 1/4)\lambda_o$ for $z > 0$, and from $-(\nu + 1/4)\lambda_o$ for $z < 0$.

With the above choice of basis and testing functions, a set of results for the reflection and transmission coefficients or, equivalently, the S-parameters, of the slot discontinuity have been obtained for a slot of dimensions 1×0.05 in. The truncation points have been chosen at three guide wavelengths from the axis of the slot. Typically, three iterations steps are sufficient to obtain convergence of the perturbational current. The results from the numerical computations are compared to measurements carried out on the network analyzer (HP 8510), and show good agreement as can be seen from Figs. 8 and 9. This agreement does, however, deteriorate at higher frequencies. This is to be expected since at these frequencies the thin-slot assumption that the x-directed electric field in the slot is negligible starts to break down. Furthermore, a more accurate description (i.e., one that would include edge effects) of the z-directed aperture field is needed at the higher frequencies in addition to a more complete representation of the

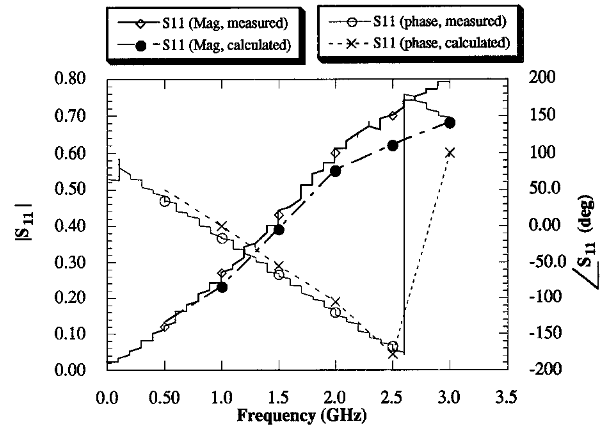

Fig. 8. Magnitude and phase of the measured and computed S_{11} for a 1×0.05 in slot.

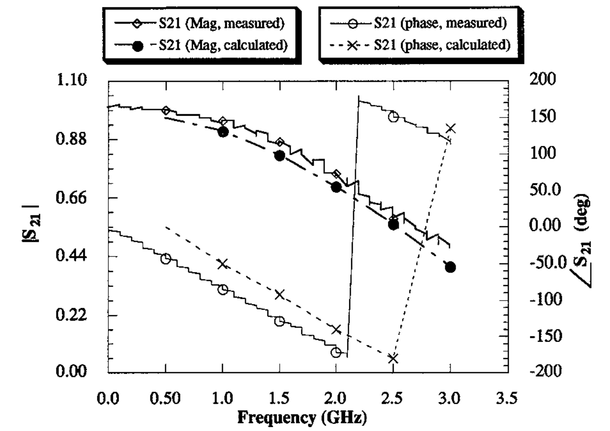

Fig. 9. Magnitude and phase of the measured and computed S_{21} for a 1×0.05 in slot.

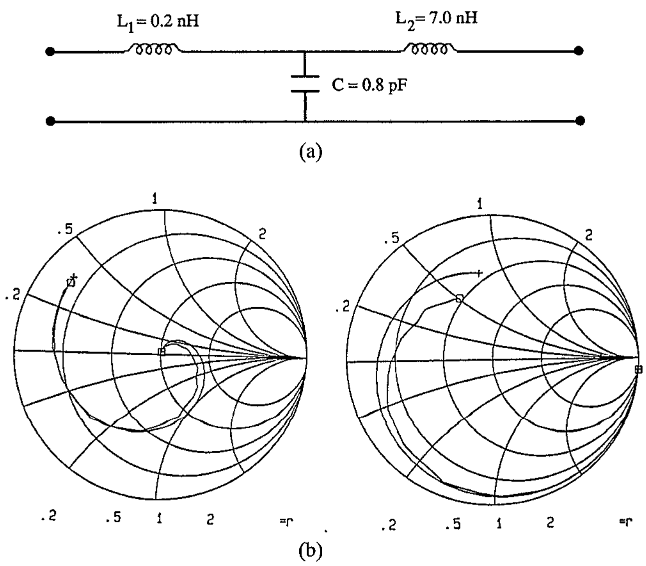

Fig. 10. Optimized equivalent circuit model for the slot of Figs. 8 and 9 for frequencies between 0.5 and 3.0 GHz. (a) Equivalent circuit; (b) □ S_{11} measured, $+S_{11}$ from equivalent circuit; (c) □ S_{21} measured, $+S_{21}$ from equivalent circuit.

microstrip currents (both x- and z-directed). These corrective measures can all be introduced with no additional efforts in the formulation process presented above. However, the real cost of eliminating the simplifying assumptions and opting instead for the fully rigorous approach is that the numerical work/resources required are more than doubled. For the frequency range considered, a simple equivalent circuit model has been obtained. Using the measured data and the circuit simulator TouchStone, the slot discontinuity was represented by a T circuit with two inductances and a capacitance placed on the microstrip line at the slots location. This circuit model, showing the values for the inductances and the capacitance obtained through a TouchStone optimization, and the corresponding scattering parameters are shown in Fig. 10.

REFERENCES

[1] A. Farrar and A. T. Adams, "Computation of lumped microstrip capacities by matrix methods: Rectangular sections and end effect," *IEEE Trans. Microwave Theory Tech.*, vol. MTT-19, pp. 495–496, 1971; correction, vol. MTT-20, p. 294, 1972.

[2] B. Easter, "The equivalent circuit of some microstrip discontinuities," *IEEE Trans. Microwave Theory Tech.*, vol. MTT-23, pp. 655–660, 1975.

[3] P. Bendek and P. Silvester, "Microstrip discontinuity capacitance for right-angle bends, T junctions, and crossings," *IEEE Trans. Microwave Theory Tech.*, vol. MTT-21, pp. 341–346, 1973.

[4] P. Anders and F. Arndt, "Microstrip discontinuity capacitance and inductance for double steps, mitered bends with arbitrary angle and asymmetric right-angle bends," *IEEE Trans. Microwave Theory Tech.*, vol. MTT-28, pp. 1213–1217, 1980.

[5] A. Khebir, A. B. Kouki, and R. Mittra, "Asymptotic boundary condition for the finite element analysis of three-dimensional transmission line discontinuities," *IEEE Trans. Microwave Theory Tech.*, vol. MTT-38, pp. 1427–1432, Oct. 1990.

[6] M. Naghed and I. Wolff, "Equivalent capacitances of coplanar waveguide discontinuities and integrated capacitors using a three-dimensional finite difference method," *IEEE Trans. Microwave Theory Tech.*, vol. MTT-38, pp. 1808–1815, Dec. 1990.

[7] I. Wolff, "The waveguide model for the analysis of microstrip discontinuities," in *Numerical Techniques for Microwave and Millimeter-Wave Passive Structures*, T. Itoh, Ed. New York, Wiley, 1989, ch. 7, pp. 447–495.

[8] T. S. Chu and T. Itoh, "Analysis of microstrip step discontinuity by the modified residue calculus technique," *IEEE Trans. Microwave Theory Tech.*, vol. MTT-33, pp. 1024–1028, Oct. 1985.

[9] P. B. Katehi and N. C. Alexopoulos, "Frequency-dependent characteristics of microstrip discontinuities in millimeter-wave integrated circuits," *IEEE Trans. Microwave Theory Tech.*, vol. MTT-33, pp. 1029–1035, Oct. 1985.

[10] T. S. Chu, T. Itoh, and Y. C. Shih, "Comparative study of mode-matching formulations for microstrip discontinuity problems," *IEEE Trans. Microwave Theory Tech.*, vol. MTT-33, pp. 1018–1023, Oct. 1985.

[11] R. Vahldieck and J. Bornemann, "A modified mode-matching technique and its application to a class of quasi-planar transmission lines," *IEEE Trans. Microwave Theory Tech.*, vol. MTT-33, pp. 916–926, Oct. 1985.

[12] R. W. Jackson and D. M. Pozar, "Microstrip open-end and gap discontinuities," *IEEE Trans. Microwave Theory Tech.*, vol. MTT-33, pp. 1036–1042, Oct. 1985.

[13] N. H. L. Koster and R. H. Jansen, "The microstrip step discontinuity: A revised description," *IEEE Trans. Microwave Theory Tech.*, vol. MTT-34, pp. 213–223, Feb. 1986.

[14] R. W. Jackson, "Full-wave, finite element analysis of irregular microstrip discontinuities," *IEEE Trans. Microwave Theory Tech.*, vol. MTT-37, pp. 81–89, Jan. 1985.

[15] S. C. Wu, H. Y. Yang, N. G. Alexopoulos, and I. Wolff, "A rigorous dispersive characterization of microstrip cross and T junctions," *IEEE Trans. Microwave Theory Tech.*, vol. MTT-38, pp. 1837–1844, Dec. 1990.

[16] P. K. Park and R. S. Elliott, "Design of collinear longitudinal slot arrays fed by boxed stripline," *IEEE Trans. Antennas Propagat.*, vol. AP-29, pp. 135–140, Sept. 1982.

[17] B. N. Das and K. K. Joshi, "Impedance of a radiating slot in the ground plane of a microstripline," *IEEE Trans. Antennas Propagat.*, vol. AP-30, pp. 922–926, Jan. 1981.

[18] M. Kominami and K. Rokushima, "Analysis of an antenna composed of arbitrarily located slots and wires," *IEEE Trans. Antennas Propagat.*, vol. AP-32, pp. 154–158, Feb. 1984.

[19] G. Elazar and M. Kisliuk, "Microstrip linear slot array antennas for X-band," *IEEE Trans. Antennas Propagat.*, vol. AP-36, pp. 1144–1147, Aug. 1988.

[20] R. I. Barnett, Jr., and R. S. Elliott, "A feasibility study of stripline-fed slots arranged as a planar array with circular grid and circular boundary," *IEEE Trans. Antennas Propagat.*, vol. AP-37, pp. 1510–1515, Dec. 1989.

[21] T. Itoh, "Spectral domain immittance approach for dispersion characteristics of generalized printed circuits," *IEEE Trans. Microwave Theory Tech.*, vol. MTT-28, pp. 733–736, July 1980.

[22] C. M. Butler, Y. Rahmat-Samii, and R. Mittra, "Electromagnetic penetration through apertures in conducting surfaces," *IEEE Trans. Antennas Propagat.*, vol. AP-26, pp. 82–93, Jan. 1978.

[23] R. W. Jackson and D. M. Pozar, "Microstrip open-end and gap discontinuities," *IEEE Trans. Microwave Theory Tech.*, vol. MTT-33, pp. 1036–1042, Oct. 1985.

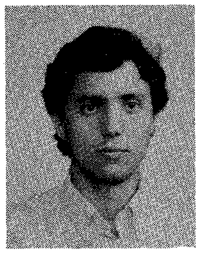

Ammar B. Kouki was born in Téboursouk, Tunisia. He received the B.S. and M.S. degrees in engineering science from the Pennsylvania State University, University Park, in 1985 and 1987, respectively, and the Ph.D. degree in electrical engineering from the University of Illinois at Urbana-Champaign in 1991.

From 1985 to 1987 he was a Research Assistant with the Research Center for the Engineering of Electronic and Acoustic Materials at the Pennsylvania State University. From 1987 to 1991 he was a Research Associate with the Electromagnetic Communications Laboratory at the University of Illinois. Since October 1991 he has been with the Microwave Research Laboratory at L'Ecole Polytechnique de Montréal. His research interests include the application of integral equation and finite element techniques to the analysis of passive microwave circuits, finite element and finite difference modeling of nonlinear devices, experimental and numerical characterization of the EMC and EMI properties of printed circuits, scattering from rough surfaces, RCS calculation, and the development of Graphical User Interfaces for electromagnetic analysis programs using X-Windows and Motif.

Dr. Kouki was the recipient of the National Scholarship from the Tunisian government from 1981 to 1991 and is a member of Tau Beta Pi.

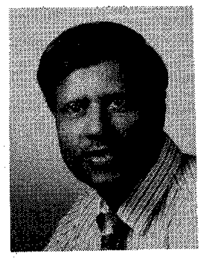

Raj Mittra is the Director of the Electromagnetic Communication Laboratory of the Electrical and Computer Engineering Department and Research Professor of the Coordinated Science Laboratory at the University of Illinois. He has been a Visiting Professor at Oxford University, Oxford, England, and at the Technical University of Denmark, Lyngby, Denmark. Currently he serves as the North American Editor of the Journal *AEÜ*. He is President of RM Associates, which is a consulting organization providing services to several industrial and governmental organizations. His professional interests include the areas of computational electromagnetics, electromagnetic modeling of electronic packaging, radar scattering, satellite antennas, microwave and millimeter-wave integrated circuits, frequency selective surfaces, EMP and EMC analysis, and remote sensing. He has published approximately 350 journal papers and 22 books or book chapters on various topics related to electromagnetics.

Dr. Mittra is a Past-President of AP-S, and has served as the Editor of the TRANSACTIONS ON ANTENNAS AND PROPAGATION. He won the Guggenheim Fellowship Award in 1965 and the IEEE Centennial Medal in 1984.

Chi Hou Chan attended Hong Kong Polytechnic and the City College of New York. He received the B.S. and M.S. degrees in electrical engineering from Ohio State University, Columbus, in 1981 and 982, respectively, and the Ph.D. degree in electrical engineering from the University of Illinois, Urbana, in 1987.

From 1981 to 1982 he was a Graduate Research Associate at the ElectroScience Laboratory, Ohio State University. From 1987 to 1989 he was a Visiting Assistant Professor with the Electromagnetic Communication Laboratory in the Department of Electrical and Computer Engineering at the University of Illinois. In September 1989 he joined the University of Washington, Seattle, as an Assistant Professor. His research interests include numerical techniques in electromagnetics, frequency selective surfaces, microwave integrated circuits, high-speed digital circuits, wave propagation in anisotropic media for integrated optics applications, finite element and finite difference methods for remote sensing and biomedical applications, and neural-networks techniques for inverse scattering and antenna designs.

Dr. Chan is a member of URSI Commission B and a recipient of the 1991 NSF Presidential Young Investigator Award.